Available online at www.sciencedirect.com

ScienceDirect

Procedia CIRP 28 (2015) 64 – 69

www.elsevier.com/locate/procedia

3nd CIRP Global Web Conference

An investigation on Nd:YAG laser cutting of Al 6061 T6 alloy sheet

C. Leone[a,b,*], S. Genna[b], A. Caggiano[a,c], V. Tagliaferri[d,b], R. Molitierno[e]

[a]*Dept of Chemical, Materials and Industrial Production Engineering, University of Naples Federico II, P.le Tecchio 80, 80125 Naples, Italy.*
[b]*CIRTIBS Research Centre, University of Naples Federico II, P.le Tecchio 80, 80125 Naples, Italy*
[c]*Fraunhofer Joint Laboratory of Excellence on Advanced Production Technology, P.le Tecchio 80, 80125 Naples, Italy*
[d]*Department of Enterprise Engineering, University of Rome Tor Vergata, Via del Politecnico 1, 00133 Rome, Italy*
[e]*MBDA Italia Spa, Via Calosi 1, 80070 Bacoli (NA) Italy*
* Corresponding author. Tel.: +39 0817682374; fax: +39 081 7682362. *E-mail address*: claudio.leone@unina.it.

Abstract

In this research work, laser cutting of 6061-T6 aluminium alloy sheets by means of a 150 W multimode pulsed Nd:YAG laser is investigated. Linear scans using the maximum average power and different cutting directions and pulse durations are executed to measure the maximum cutting speeds. Then, cutting tests are performed by varying beam travel direction, pulse duration and cutting speed. The results show that a 150W multimode pulsed Nd:YAG laser allows to cut 1 mm-thick 6061-T6 sheets with cutting speed up to 700 mm/min, obtaining narrow kerfs (< 200 μm) with a good taper angle (< 5°) and low dross height (about 40 μm).

Selection and peer-review under responsibility of the International Scientific Committee of the "3rd CIRP Global Web Conference" in the person of the Conference Chair Dr. Alessandra Caggiano.

Keywords: Pulsed laser cutting; 6061aluminium alloy; Kerf geometry; ANOVA; Design of experiment

1. Introduction

Aluminium alloys are widely used in several advanced manufacturing industries due to their unique performance related to light weight, high strength and stiffness to weight ratio and high corrosion resistance. Aluminium can be easily machined through different removal processes, but the most common and fast process for cutting complex geometries is laser cutting [1-2]. Compared to traditional processes, the latter offers several advantages, like: absence of mechanical contact and tool wear, no need for complex fixtures, possibility to create complex shapes and accurate geometries with narrow kerfs on almost all categories of materials including metals, nonmetals, ceramics and composites [1-9]. Laser cutting processes are based on thermal interaction: when the beam impacts on the material, part of the laser radiation is absorbed causing melting, vaporization or chemical state change of the material which can be easily removed by a pressurized assistant gas jet. Laser cutting of aluminium can be hard due to its reflectivity and high thermal conductivity, that tend to shed heat. Therefore, particular attention must be paid to ensure an adequate quality of the laser cut. In the literature there are a limited number of papers on laser cutting of aluminium [10-14]. Many of them concern cutting of 2-xxx or 5-xxx alloy series, while no studies on the 6-xxx alloy series are reported.

Within the 6-xxx alloy series, 6061 alloys are of high interest for advanced industries like aerospace, automotive, marine, electrical, chemical, food processing and sport equipments. These alloys have medium to high strength, medium fatigue strength and a very good corrosion resistance. They are weldable although strength is reduced in the weld zone.

In this research work, laser cutting of 6061 T6 aluminium alloy sheets through the employment of a 150 W multimode pulsed Nd:YAG laser is investigated. Two experimental test series were carried out. First, linear scans using the maximum average power (150W) and different cutting directions and pulse durations were executed. On the basis of these tests, the maximum cutting speeds were determined. In the second experimental test series, cutting tests were performed by varying the beam travel direction, the duration and the cutting speed (selected as a percentage of the maximum

Selection and peer-review under responsibility of the International Scientific Committee of the "3rd CIRP Global Web Conference" in the person of the Conference Chair Dr. Alessandra Caggiano.
doi:10.1016/j.procir.2015.04.012

cutting speed). The obtained kerfs sections were investigated by optical analysis. The upper kerf, down kerf, taper angle and dross height were measured. ANalysis Of VAriance was applied in order to study the influence of the process parameters on the kerf geometry.

2. Experimental setup

2.1. Equipment

The experimental tests were performed using a 150 W lamp pumped Nd:YAG laser (Rofin StarCut 150). The laser beam was moved by means of a CNC system (Rofin finecut Y 340M). A cutting head (Precitek AK-YK 52), equipped with a lens having a focal length of 80 mm, was mounted on the system. In this way, a focal spot of about 160 µm was obtained. In Fig. 1, a scheme of the laser system is illustrated.

The system controls the generation of the geometric patterns, the cutting speed (Cs) and the laser source process parameters: lamp voltage (V), pulse duration (D) and pulse frequency (F). Table 1 shows the detailed characteristics of the laser system.

Fixed the lamp voltage at the maximum value, the average power (Pa) depends on the adopted values of D and F, as reported in Fig. 2. The average power was measured using a power meter (F150A-SH thermal head and NOVA display by OPHIR). By observing Fig. 2, it can be noticed that, for a fixed pulse duration, average power increases according to the increase of pulse frequency until reaching a plateau value. From there on, a decrease of average power is seen.

In this type of laser, the selection of the process parameters is a critical issue because the maximum cutting speed depends on the average power, but also on pulse energy (Pe) and pulse power (Pp). Furthermore, Pe and Pp play a central role in laser machining and micromachining as they determine, together with the focus spot, the fluence (energy density) and the irradiance (power density) and so the laser beam-material interaction mode, the amount of machined volume and the kerf geometry [1-9, 13-14].

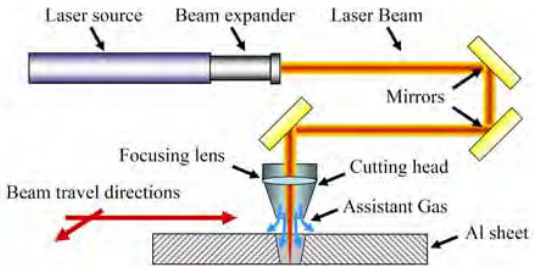

Fig. 1. Scheme of the laser system

Table 1. Laser system characteristics.

Characteristic	Symbol	Value	Units
Wavelength	λ	1064	[nm]
Average nominal Power	Pa	150	[W]
Pulse duration	D	0,03÷2,5	[ms]
Pulse frequency	F	up to 3	[kHz]
Mode	--	Multimode	
Focal length of focussing lens	--	80	[mm]
Focused spot diameter	--	160	[µm]

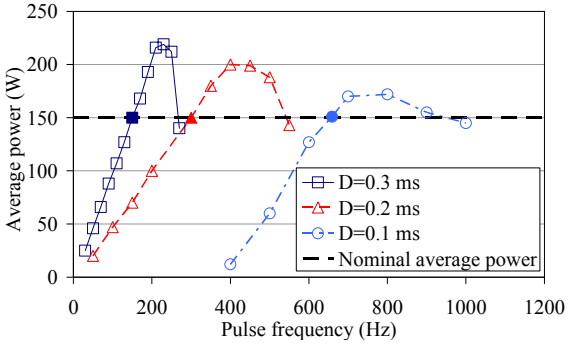

Fig. 2. Average power as a function of the pulse frequency at different durations. Data obtained with a lamp voltage of 700 V. The filled points represent the adopted frequency.

Pe and Pp depend on the process parameters Pa, D and F according to the well known equations:

$$Pe = Pa / F \tag{1}$$

$$Pp = Pe / D = Pa / (F \cdot D) \tag{2}$$

At the same time, it is worth noting that frequency (F) in conjunction with cutting speed (Cs) controls the superposition of two pulses in space and time domains, the so-called overlapping, that is an additional critical parameter for pulse laser applications.

The overlapping percentage can be calculated through the following equation:

$$R\% = \left[1 - \left(Cs / F \cdot ds\right)\right] \cdot 100 \tag{3}$$

where *ds* is the spot diameter on the components.

In the adopted laser system, due to the multimode nature of the source, the laser spot is elliptical. As a result, the overlapping factor and the beam footprint width vary along with the beam travel direction, as visible in Fig. 3. Accordingly, also the maximum cutting speed and the kerf width vary with the beam travel direction.

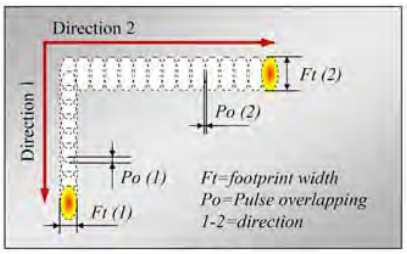

Fig. 3. Effect of the elliptical spot shape on the overlapping factor and on the kerf width as a function of the beam travel direction.

2.2. Material

The investigated material is 6061-T6 aluminium alloy (UNS A96061; ISO AlMg1SiCu) in the form of 1 mm-thick rolled sheets. Al-6061 is a precipitation hardening aluminium alloy containing magnesium and silicon as major alloying elements; it is usually adopted in aircraft structures, automotive parts, yachts, boats and scuba equipments due to its workability, weldability and corrosion resistance. In Table 2, the chemical composition and the main properties of the 6061-T6 alloy are reported [15].

2.3. Experimental procedure

Two experimental testing series were performed. First, to obtain the maximum cutting speed (Sl), i.e. the speed beyond which it is not possible to cut the sheet, 30 mm-long linear scans were carried out with the laser beam focused on the surface and maximum average power (150 W) while varying beam travel speed (mm/s), pulse duration and beam direction.

Table 2. Chemical composition and properties of Al6061-T6 [15]

Element	Al	Mg	Si	Cr	Mn
min [%]	95.8	0.8	0.4	0.04	--
max [%]	98.6	1.2	0.8	0.35	0.15
Element	Cu	Fe	Zn	Ti	Other
min [%]	0.15	--	--	--	--
max [%]	0.4	0.7	0.25	0.15	0.05

Physical and mechanical properties		Value	Units
Density		2.7	[g/cm^3]
Melting Range:	Liquidus temperature	582	[°C]
	Solidus temperature	652	
Specific Heat		0.896	[J/kg,°C]
Thermal Conductivity		167	[W/m°C]
Tensile Strength		310	[MPa]
Yield Strength (at 0.2%)		276	[MPa]
Elongation		12-17	[%]
Young's modulus		68.9	[GPa]

For these tests, the process parameters were selected according to the above mentioned considerations made on Pe and Pp. In particular, duration was chosen so as to take into account the possible influence of Pe or Pp on the process. Therefore, in this first phase, three different values of duration were adopted and pulse frequency was selected in order to have a Pa value equal to the nominal value (150W). On the other hand, the direction was chosen so as to take into account the effect of energy distribution. In Table 3, the process parameters adopted for the evaluation of the maximum cutting speed are reported.

Afterwards, a second testing series was performed to verify the influence of the process parameters on the kerf geometry. For this experimental phase a 2^2x3 full factorial design was developed according to the Design of Experiments (DoE) methodology. The following control factors were adopted: duration, maximum cutting speed and beam travel direction. In particular, it was chosen to adopt a Sl corresponding to the 100% and 90% and 80% of the minimum Sl measured for the two directions and for each duration, the maximum and the minimum durations adopted in the first test, and the two directions. These conditions were adopted considering the effect of duration described below and the fact that, from a practical point of view, neither it is conceivable to use the highest speed (which would not assure cutting along all the directions), nor to change the speed along with the cutting direction. For each treatment, 4 replications were executed. Table 4 summarizes the levels of the control factors and their settings.

In order to determine which of the process parameters affect the kerf geometry and how, Analysis Of Variance (ANOVA) was used. The analysis was carried out at a 95% confidence level (α=0.05), and the p-value was used to determine the significance of the factors or their combinations. Thus, a single process parameter or an interaction is significant if the *p*-value is less than 0.05. The MiniTab R.16 software tool was adopted for the analysis. After the tests, the samples were cut, included in epoxy resin and then polished using abrasive paper of grit size up to P2500 (Standard ISO 6344). Then, images of the kerf sections were taken by optical microscopy (Zeiss Axioskop 40) and the geometry was measured according to the UNI EN ISO 12584 standard. In particular, the kerf width at the inlet of the beam, called upper kerf (Uk), and at the exit of the beam, called down kerf (Dk) and the dross height (Dh) were measured. Fig. 4 shows a scheme of the kerf section and how Uk, Dk and Dh were measured.

In addition, after measuring, the taper angle (Ta) was calculated via the following equation:

$$Ta = \tan^{-1}\left[(Uk - Dk)/(2 \cdot t)\right] \quad (4)$$

Where, in the equation, t is the sheet thickness.

Table 3. Process conditions and tested samples

Control factors	Labels	Low (−)	Midle (0)	High (+)	Unit
Direction	Dr	1	--	2	--
Duration	D	0.1	0.2	0.3	[ms]
Cutting speed	**up to incomplete cut**				

Table 4. Control factors adopted in the kerf analysis

Control factors	Labels	Low (−)	Midle (0)	High (+)	Unit
Direction	Dr	1	--	2	--
Speed limit	Sl	80	90	100	[%]
Duration	D	0.1	--	0.3	[ms]

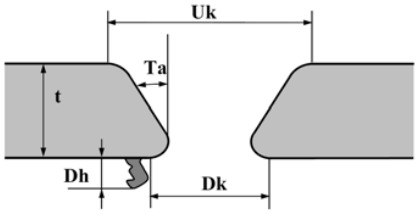

Fig. 4. Definition of kerf geometry parameters (UNI EN ISO 12584)

3. Experimental results and discussion

3.1. Maximum cutting speed

In Fig. 5, the maximum cutting speed is reported as a function of duration (D) for both directions (Dr). It can be observed that the maximum cutting speed linearly increases at the increase of pulse duration. Furthermore, as it was expected, it increases moving from direction 2 to direction 1. The results clearly indicate the effect of pulse duration (the maximum cutting speed decreases if the D is decreased) and also clarify the choices made in the DoE development.

Since the cutting pattern is not made of straight lines, and it is arranged along the two directions, it is not advisable to use the maximum speed. Neither it is possible to think to adjust the cutting speed as a function of direction. Therefore, to ensure the cut on any geometry, the use of the lowest speed among those guaranteed in both directions it is necessary. In Table 5 the process parameters (D, F, Pp and Ep), the maximum cutting speed (100% Sl), and the absolute values of the Sl adopted for the second experimental test are reported.

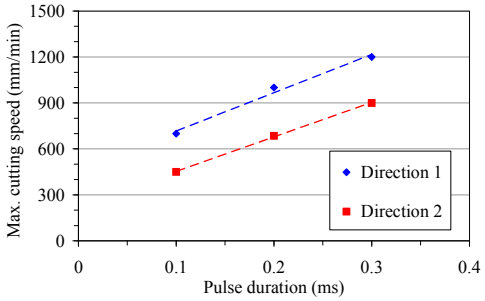

Fig. 5. Maximum cutting speed as a function of pulse duration for the two beam travel directions

Table 5. Process parameters, maximum cutting speed and the absolute values of the Sl adopted for the second experimental test

D	F	Pp	Ep	Cutting speed [mm/s]*		
[ms]	[Hz]	[kW]	[J]	100% Sl	90% Sl	80% Sl
0.3	150	3.33	1.00	900	810	720
0.1	659	2.28	0.23	450	405	360

3.2. Kerf geometry

ANOVA assumes that the observations are normally and independently distributed with the same variance for each treatment or factor level. Then, before the analysis, the ANOVA assumptions have been successfully checked via graphical examination of residuals, in agreement with what reported in [16]. However, these results were not reported here for sake of briefness. In Table 6, the ANOVA results are summarized in terms of p-values. From the table and on the basis of the assumptions (α=0.05), the direction affects both the kerf widths and the taper angle, the duration affects the down kerf, the taper angle and the dross height. The maximum cutting speed (Sl) does not affect any response variables. It is unexpected, probably it is due to the use of too closest values for Sl. Regarding the two way interaction, ANOVA indicates, as significant, the interaction Dr*D for Uk, Dk, and Ta.

Table 6. ANOVA results, p-value

Control factor Source	Upper kerf	Down kerf	Taper angle	Dross height
Dr	**0.000**	**0.000**	**0.000**	0.272
D [ms]	0.115	**0.000**	**0.000**	**0.000**
Sl [%]	0.562	0.484	0.232	0.140
Dr*D	**0.047**	**0.034**	**0.002**	0.140
Dr*Sl	0.567	0.353	0.165	0.242
Sl*Dr	0.816	0.922	0.975	0.840
Dr*D*Sl	0.879	0.111	0.199	0.063

The main effects plots and the interaction plots reported in Figs. 6-12 help understand the effect of the significant factors. In the main effects plots (Figs. 6-9) the significant factors are highlighted using continuous lines. In the interaction plots (Figs. 10-12) only the statistically significant interactions are reported.

In Fig. 6a, the main effects plot for Uk shows that the upper kerf decreases moving from direction 1 to 2. The highest kerf width obtained in direction 1 is probably due to the fact that in this direction the laser beam works at a Sl% lower than the real Sl (Fig. 5). Consequently, the molten material increases and the upper kerf is enlarged. This effect is more evident when the duration has a low value, as visible in the two-way interaction plot of Fig. 10b. The opposite happens for the down kerf, Fig. 7a: this because the high amount of molten material produced as the laser beam travels along direction 1 tends to solidify at the bottom of the kerf due to the high thermal conductivity of the aluminium alloy, thus reducing the down kerf width. Obviously, the opposite occurs in direction 2. This effect is more evident when pulse duration is set to 0.1 ms (Fig. 11b). The effect of pulse duration on Dk is due to similar phenomena, Fig. 7b. An increase of pulse duration produces an increase of the molten material and higher temperatures of molten and solid materials in the kerf. This allows the gas to easily expel the molten material from the kerf. This effect is more evident when the beam travels along direction 1 (Fig. 11a). The taper angle is affected by both Uk and Dk: in particular, it decreases going from direction 1 to 2 (Fig. 8a) and when duration increases (Fig. 8b). Similarly to the behaviour of Uk and Dk, also in this case the effects of direction and duration are more evident when duration is set at a low value (Fig. 12b) or the beam travels along direction 1 (Fig. 12a). The dross height is affected by duration only, Fig. 9b, as a consequence of the previously described behaviour: as duration increases, the amount of molten material is more easily expelled from the kerf section. However, part of the molten material tends to remain attached to the bottom edge of the kerf, thus forming the dross.

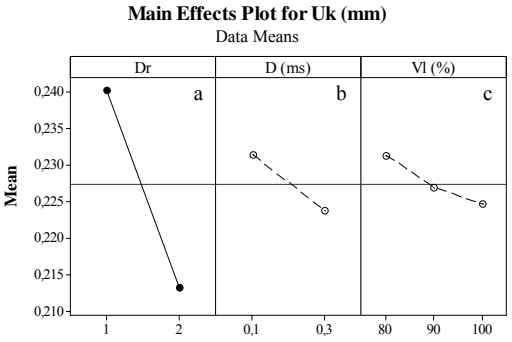

Fig. 6. Main effects plot for upper kerf (Uk)

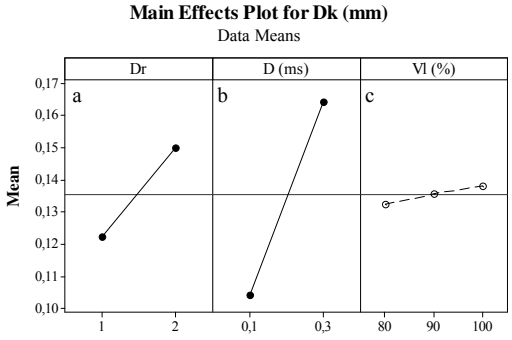

Fig. 7. Main effects plot for down kerf (Dk)

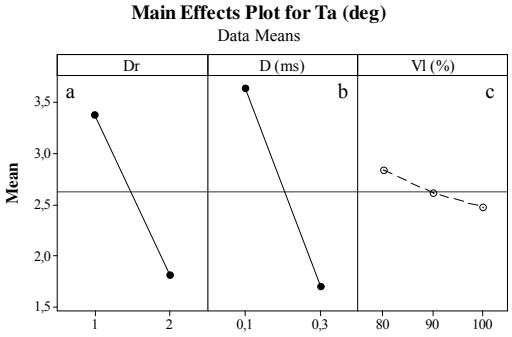

Fig. 8. Main effects plot for taper angle (Ta)

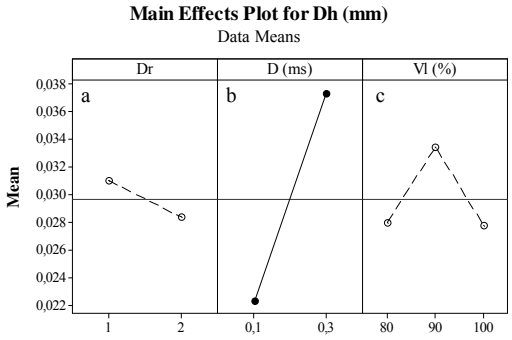

Fig. 9. Main effects plot for dross height (Dh)

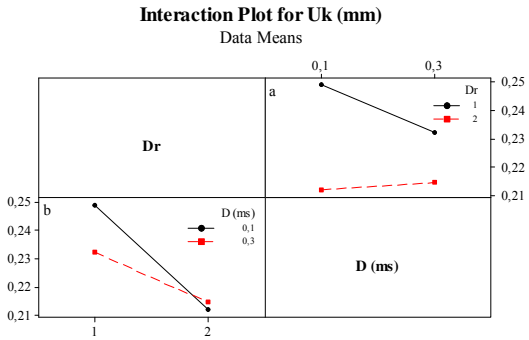

Fig. 10. Interaction plot for upper kerf (Uk)

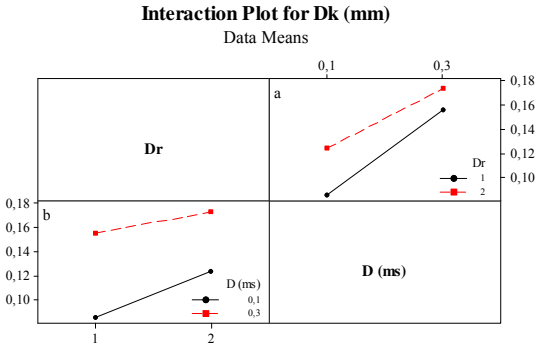

Fig. 11. Interaction plot for down kerf (Dk)

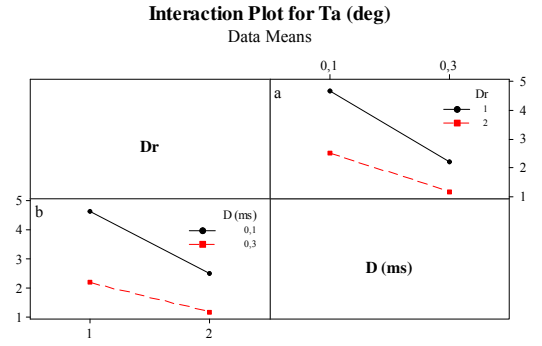

Fig. 12. Interaction plot for taper angle (Ta)

4. Conclusions and future developments

Laser cutting tests were performed on 1 mm-thick 6061-T6 aluminium alloy sheets adopting a 150W multimode pulsed Nd:YAG laser to study the influence of the process parameters on the kerf geometry. Two experimental test plans were developed and performed. The first was used to measure the maximum cutting speed at the maximum average power. The maximum cutting speed varies in the range 1200÷450 mm/min depending on beam travel direction and pulse duration. It increases with a longer pulse duration and when the laser beam travels along the minor axis of the elliptical focus footprint.

In the second test series, the effects of beam travel direction, pulse duration and cutting speed (selected as a percentage of the maximum cutting speed) on the kerf geometry were investigated by means of ANOVA. The beam travel direction affects both the kerf widths and the taper angle. The pulse duration affects the down kerf, the taper angle and the dross height. From a practical point of view, a nearly perpendicular kerf (Ta<4°) can be obtained adopting a long pulse duration. In this condition, a dross height lower than 40 μm is obtained.

In order to provide a complete assessment of the kerf quality, a characterization of the HAZ extension and the roughness measured along the kerf would be advisable. This aspect needs further studies and it will be investigated in a future research activity.

Acknowledgements

The authors gratefully acknowledge the CIRTIBS Research Centre of the University of Naples Federico II and MBDA Italia Spa for providing the equipment, the materials and the technical support necessary to the development of this research work.

References

[1] Salonitis, K., Stournaras, A., Tsoukantas, G., Stavropoulos, P., Chryssolouris, G., 2007. A Theoretical and Experimental Investigation on Limitations of Pulsed Laser Drilling, J. of Material Processing Technology, 183, p. 96-103.
[2] Dubey, A.K., Yadava, V., 2008. Laser beam machining - a review, Int. J. of Machine Tools and Manufacture 48, p. 609-28.
[3] Astarita, A., Genna, S., Leone, C., Memola C.M., F., Paradiso, V., Squillace, A., 2013. Ti-6Al-4V cutting by 100W fibre laser in both CW and modulated regime, Key Engineering Materials 554-557, p. 1835-1844.
[4] Morace R.E., Leone C., De Iorio I., Cutting of thin metal sheets using Nd:YAG lasers with different pulse duration, Proceedings of SPIE, 2006; 6157: Article number 61570Q.
[5] Astarita A., Genna S., Leone C., Minutolo.F., Paradiso V, Squillace A., 2014, Laser Cutting of Aluminium Sheets with a Superficial Cold Spray Titanium Coating, Key Engineering Materials,, 611 – 612, p. 794-803.
[6] Tonshoff, H.K., Emmelmann, C., 1989, Laser Cutting of Advanced Ceramics, CIRP Annals 38, p. 219-222.
[7] Quintero, F., Pou, J., Lusquiños, F., Boutinguiza, M., Sot, R., Pérez-Amor, M., 2001. Nd:YAG laser cutting of advanced ceramics, Proceedings of SPIE 4419, p. 756-760.
[8] Leone, C., Pagano, N., Lopresto, V., De Iorio, I., 2009. Solid state Nd:YAG laser cutting of CFRP sheet: influence of process parameters on kerf geometry and HAZ, 17th Int. Conf. on Composite Materials - ICCM-17, July 27-31, Edinburgh, UK, Code 85394.
[9] Leone, C., Genna, S., Tagliaferri, V., 2014. Fibre laser cutting of CFRP thin sheets by multi-passes scan technique, Optics and Lasers in Engineering 53, p. 43-50.
[10] Dubey, A.K., Yadava, V., 2008, Optimization of kerf Quality During Pulsed Laser Cutting of Aluminum Alloy Sheet, J. of Materials Processing Technology, 204, p. 412-418.
[11] Riveiro A. , Quintero F., Lusquiños F., Pou J., Pérez-Amor M., Laser cutting of 2024-T3 aeronautic aluminum alloy, J. of Laser Applications, 2008; 20/4: 230-235.
[12] Stournaras, A., Stavropoulos, P., Salonitis, K., Chryssolouris, G., 2009. An investigation of quality in CO_2 laser cutting of aluminum, CIRP J. of Manufacturing Science and Technology 2, p. 61-69.
[13] Sharma, A., Yadava, V., 2012. Modelling and optimization of cut quality during pulsed Nd:YAG laser cutting of thin Al-alloy sheet for straight profile, Optics and Laser Technology 44/1, p. 159-168.
[14] Sharma, A., Yadava, V., 2013. Modelling and optimization of cut quality during pulsed Nd:YAG laser cutting of thin Al-alloy sheet for curved profile, Optics and Lasers in Engineering 51/1, p. 77-88
[15] Metals Handbook, Vol.2 - Properties and Selection: Nonferrous Alloys and Special-Purpose Materials, ASM International 10th Ed. 1990.
[16] Montgomery, D.C., 2008. Design and Analysis of Experiments., New York, Wiley.